

pubs.acs.org/acssensors Article

Flexible Chemiresistive Cyclohexanone Sensors Based on Single-Walled Carbon Nanotube-Polymer Composites

Bora Yoon, [⊥] Seon-Jin Choi, [⊥] Timothy M. Swager,* and Gary F. Walsh*



Cite This: ACS Sens. 2021, 6, 3056-3062



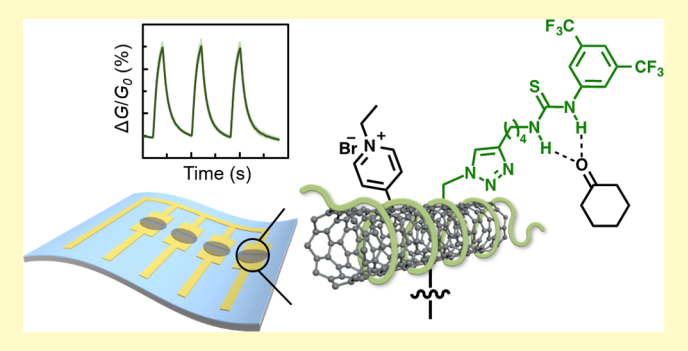
ACCESS

Metrics & More

Article Recommendations

s Supporting Information

ABSTRACT: We report a chemiresistive cyclohexanone sensor on a flexible substrate based on single-walled carbon nanotubes (SWCNTs) functionalized with thiourea (TU) derivatives. A wrapper polymer containing both 4-vinylpyridine (4VP) groups and azide groups (P(4VP-VBAz)) was employed to obtain a homogeneous SWCNT dispersion via noncovalent functionalization of SWCNTs. The P(4VP-VBAz)—SWCNT composite dispersion was then spray-coated onto an organosilanized flexible poly(ethylene terephthalate) (PET) film to achieve immobilizing quaternization between the pyridyl groups from the polymer and the functional PET substrate, thereby surface anchoring SWCNTs. Subsequent surface functionalization was performed to incorporate



a TU selector into the composites, resulting in P(Q4VP-VBTU)—SWCNT, for the detection of cyclohexanone via hydrogen bonding interactions. An increase in conductance was observed as a result of the hydrogen-bonded complex with cyclohexanone resulting in a higher hole density and/or mobility in SWCNTs. As a result, a sensor device fabricated with P(Q4VP-VBTU)—SWCNT composites exhibited chemiresistive responses ($\Delta G/G_0$) of 7.9 \pm 0.6% in N₂ (RH 0.1%) and 4.7 \pm 0.4% in air (RH 5%), respectively, upon exposure to 200 ppm cyclohexanone. Selective cyclohexanone detection was achieved with minor responses ($\Delta G/G_0$ < 1.4% at 500 ppm) toward interfering volatile organic compounds (VOC). analytes. We demonstrate a robust sensing platform using the polymer—SWCNT composites on a flexible PET substrate for potential application in wearable sensors.

KEYWORDS: carbon nanotubes, cyclohexanone sensing, chemiresistor, copolymer, PET, flexible substrate

Trace detection of explosives is important in countering weapons of mass destruction. There has been a growing demand for selective and sensitive detection of explosives for aviation security and ground package screening as well as for warfighters on the battlefield. Explosive traces are typically detected by sampling vapors or residue particulates left on surfaces, and analyzing them with analytical methods such as ion mobility spectrometry, mass spectrometry, gas chromatography, and optical spectroscopy. Although the current methods provide high sensitivity and selectivity, they are cumbersome, expensive, and often require skilled operators. Therefore, it is desirable to develop explosive trace detectors that are accurate, inexpensive, rapid, portable, and easy to deploy with minimal training.

One of the most common energetic substances in plastic explosive formulations is cyclotrimethylenetrinitramine (RDX). As a result of its low vapor pressure at room temperature, RDX sensing can be conducted by detecting cyclohexanone, a nonexplosive vapor that is a residue from the recrystallization of RDX. Previous efforts toward selective detection of cyclic ketone vapors for RDX sensing include the use of fluorescent dyes, colorimetric arrays, ionic liquids, metal—organic frameworks, arrays, carbon nanotubes. Among these materials, single-walled carbon

nanotubes (SWCNTs) have been recognized as excellent chemical-sensing materials that display sensitive resistance changes to target analytes with proper functionalization. $^{18-24}$ In that regard, our group has previously reported on cyclohexanone chemiresistive sensors based on SWCNTs functionalized with a thiourea moiety, capable of binding cyclohexanone via hydrogen bonding interaction. 15,16 Although it has been demonstrated that covalently or noncovalently functionalized SWCNT—thiourea composites facilitate selective detection of trace cyclohexanone, the former inevitably disrupts the extended π -electronic states in the nanotube sidewalls. To avoid this electronic perturbation to the SWCNTs, noncovalent functionalization is preferred, but this approach often results in composites with low stability that limit sensing performance and applications. 19

Received: May 24, 2021 Accepted: July 27, 2021 Published: August 6, 2021





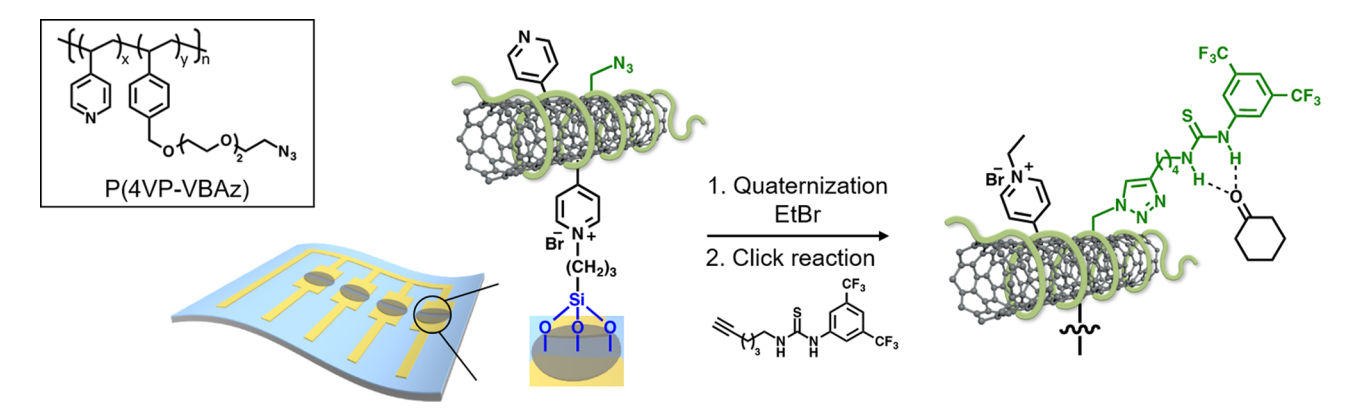


Figure 1. Schematic illustration of surface functionalization for a chemiresistive cyclohexanone sensor on a flexible PET substrate.

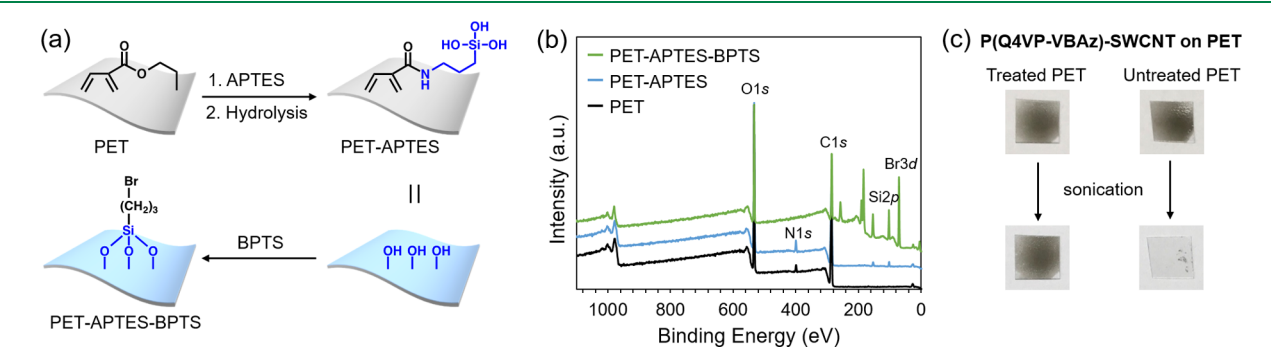


Figure 2. (a) Schematic illustration of the surface functionalization process of a PET substrate. (b) XPS survey spectra of bare PET, PET-APTES, and PET-APTES-BPTS. (c) Photographs of the spray-coated P(Q4VP-VBAz)—SWCNT composites on treated and untreated PET films, respectively, and photographs after sonication for 1 min in dichloromethane.

Here, we describe the adaptation of a modular SWCNT chemiresistive sensor platform from our previous research, wherein SWCNT dispersions stabilized with a poly(4-vinyl pyridine) (P4VP) wrapper, or a copolymer thereof, are covalently immobilized onto a glass substrate and functionalized with an analyte selector. We hypothesized that surface-anchored SWCNT composites functionalized with a thiourea selector can address the aforementioned limitations of noncovalent functionalization and provide stable chemiresistive sensing performance for cyclohexanone.

We first prepared a SWCNT composite with a wrapper copolymer, P(4VP-VBAz), containing both 4VP groups and azide groups (Figure 1).²⁸ To demonstrate the versatility of our approach, we fabricated a sensor device on a surface-functionalized flexible poly(ethylene terephthalate) (PET) substrate, wherein the 4VP groups of the SWCNT composites undergo a nucleophilic substitution reaction with surface alkyl bromides. We then further quaternized the residual pyridyl groups with bromoethane and subsequently introduced the thiourea groups via a "click" reaction to produce P(Q4VP-VBTU)–SWCNT composites for cyclohexanone detection (Figure 1). The flexible chemiresistive cyclohexanone sensor showed a reversible response with enhanced sensitivity to cyclohexanone. In addition, the results confirm that our modular polymer-wrapped SWCNTs create a versatile and robust chemiresistive sensor platform for target analytes.

RESULTS AND DISCUSSION

The surface functionalization of a chemiresistive cyclohexanone sensor on a flexible PET substrate is illustrated in Figure 1. The precursor wrapper polymer P(4VP-VBAz)

bearing both 4VP and azide groups was synthesized via free radical polymerization as reported previously, 28 and is detailed in the Supporting Information. The polymer molecular weight determined by gel permeation chromatography is 33.90 kDa with a $M_{\rm w}/M_{\rm n}$ of 2.08 (Figure S1a). The molar ratio between 4VP and azide tethered groups was found to be 10:1 based on NMR characterization (Figure S1b). We prepared a stable P(4VP-VBAz)-SWCNT dispersion by sonicating a mixture of polymers (50 mg) and CoMoCAT SWCNTs with an average diameter of 0.82 nm (10 mg) in DMF (10 mL) for 1 h in an ultrasonic bath chilled with ice, followed by centrifugation for 30 min at 15,000g to remove solids. The isolated supernatant from the centrifuged suspension shows highly concentrated SWCNTs (Figure S2a). A sharp structured UV-vis-NIR spectrum of the P(4VP-VBAz)-SWCNT dispersion (1:3 dilution in DMF) further confirms that nanotubes are individually debundled and stabilized through favorable interactions between the pyridyl SWCNT dispersant groups of the polymer and SWCNT sidewalls (Figure S2b). The dispersion was stable for prolonged periods (>2 months) when stored on the benchtop at room temperature.

In order to demonstrate the versatility of our approach on a flexible substrate, we introduced alkyl bromide moieties on the PET surface to covalently anchor the P(4VP-VBAz)–SWCNT composites via an immobilizing quaternization. The surface modification of PET with 3-aminopropyltriethoxysilane (APTES) has been reported to create silica-like surface functionalities, wherein the APTES primary amine undergoes an amidation reaction and subsequent hydrolysis produces a silanol surface. 31–34 Fadeev and McCarthy have previously reported PET modification procedures using APETS and

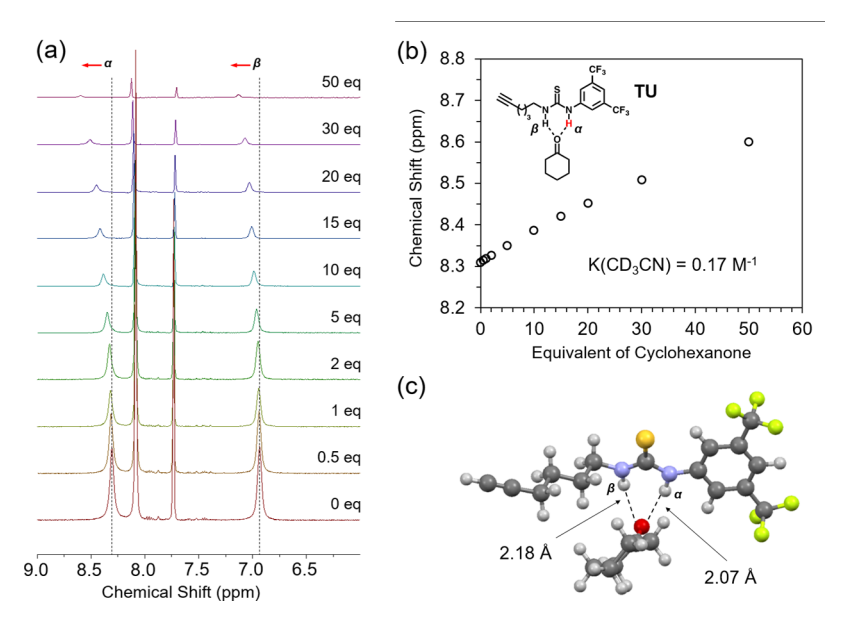


Figure 3. (a) ¹H NMR chemical shifts of the thiourea NH protons (α and β) of TU upon addition of increasing concentrations of cyclohexanone (0–50 equiv). (b) Plot of ¹H NMR chemical shifts of the thiourea NH proton (α) (highlighted in red in the inset) upon addition of cyclohexanone. (c) DFT optimized molecular structure of the TU and cyclohexanone complex.

confirmed each step of surface by water contact angle measurements, which showed the increase in hydrophilicity of the silanol-modified PET surface.³¹ We have followed the literature procedures with slight modifications to create a silanol surface on PET, then treated with 3-bromopropyltrichlorosilane (BPTS) to generate surface-bound alkyl bromide groups (Figure 2a). The brief procedure is as follows: a PET film is immersed in APTES solution in dry toluene (1:10, v/v) at 80 °C for 2 days. After subsequent hydrolysis of triethoxysilane terminal groups in acidic water (pH 5) for 1 h, the film is functionalized by immersion in a dry toluene solution of BPTS (1:10, v/v) overnight at room temperature under dry nitrogen atmosphere. The PET surface functionalization was confirmed by X-ray photoelectron spectroscopy (XPS) analysis shown in Figure 2b. The XPS survey spectrum of an untreated commercial PET sample revealed the presence of trace nitrogen with 2.3 at. % N 1s on the surface, which could be attributed to manufacturing additives. After the APTES treatment followed by hydrolysis, the Si 2p peak and increased N 1s peak intensity (4.2 at. %) were observed in the XPS spectrum of PET-APTES, indicating the incorporation of APTES to the PET surface. The introduction of alkyl bromide groups was confirmed by the Br 3d peak (13.7 at. %) in the PET-APTES-BPTS spectrum. The N 1s peak was not observed for the resulting functionalized PET surface, which reveals that the top BPTS layer attenuates the emission of elastic electrons from the nitrogen groups. Detailed surface chemical composition in at. % from the XPS data of the PET films is summarized in Table S1. To assess the surface anchoring of polymer-SWCNT composites on the PET-APTES-BPTS film, 0.5 mL of the P(4VP-VBAz)-SWCNT dispersion was loaded into an airbrush and manually sprayed onto the PET-APTES-BPTS film placed on a 130 °C hot plate. After overnight thermal annealing at 60 °C to ensure the quaternization of 4VP groups with the PET functional surfaces, the film was sonicated in pure dichloromethane for 1 min to remove excess polymers and non-immobilized polymer-SWCNT composites. As shown in Figure 2c, a significant amount of the P(4VP-

VBAz)—SWCNT composite remains on the treated PET substrate, whereas the composite sprayed and treated similarly onto untreated bare PET only retained a trace amount of physisorbed composite after the sonication.

To create a cyclohexanone selector on the flexible P(4VP-VBAz)-SWCNT precursor platform, we first synthesized a thiourea (TU) containing a 6-hexynyl group for click chemistry and an electron-withdrawing 3,5-bis-(trifluoromethyl)phenyl group for increased acidity of the thiourea NH protons^{15,16} (synthetic details in the Supporting Information). We performed ¹H NMR binding studies and density functional theory (DFT) calculations with TU and cyclohexanone to determine the binding details (Figure 3). The ¹H NMR titrations in acetonitrile-d₃ revealed a downfield shift of the TU NH protons upon complexation with cyclohexanone, thus confirming the expected two point hydrogen bonding with cyclohexanone (Figure 3a). The chemical shifts of the TU NH_a to the 3,5-bis(trifluoromethyl)phenyl group were used to calculate an equilibrium constant (K) of 0.17 M^{-1} (Figure 3b). The optimum geometry of the TU-cyclohexanone complex obtained by DFT calculations is shown in Figure 3c. The favorable complex of TU-cyclohexanone is confirmed with a free energy change (ΔG) of -2.76 kcal/mol and the bond distances of 2.07 Å for H_a ...O and 2.18 Å for H_{β} ···O. A shorter distance of the H_{α} ···O bond is attributed to the electron-withdrawing 3,5-bis-(trifluoromethyl)phenyl moiety, which creates a more acidic NH proton.

Chemiresistive cyclohexanone sensors were fabricated by spray-coating a P(4VP-VBAz)-SWCNT dispersion on a heated PET-APTES-BPTS substrate. The residual pyridyl groups that are not consumed in the immobilizing quaternization, were functionalized with bromoethane. The latter liberates hole charge carriers in the SWCNTs, which were pinned by the lone pairs of 4VP. Alkylation removes the donating lone pairs and enhances the hole transport in the SWCNTs. Finally, the TU substituent was introduced to the surface-immobilized composite via a click reaction to form

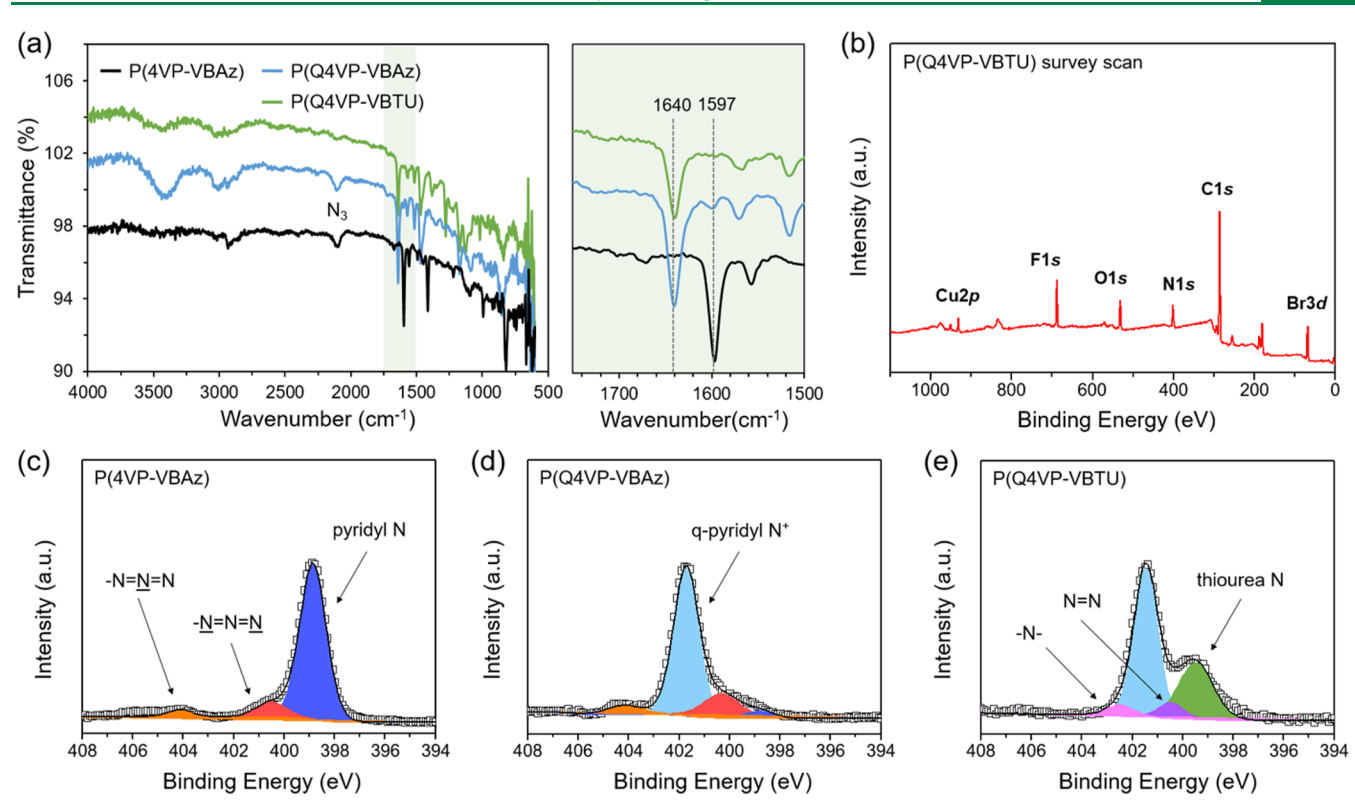


Figure 4. (a) ATR-FTIR spectra of the polymer–SWCNT composite films on PET substrates. (b) XPS survey spectrum of the P(Q4VP-VBTU)–SWCNT film. High-resolution XPS spectra of N 1s of (c) P(4VP-VBAz)-SWCNT, (d) P(Q4VP-VBAz)-SWCNT, and (e) P(Q4VP-VBTU)-SWCNT films on PET substrates.

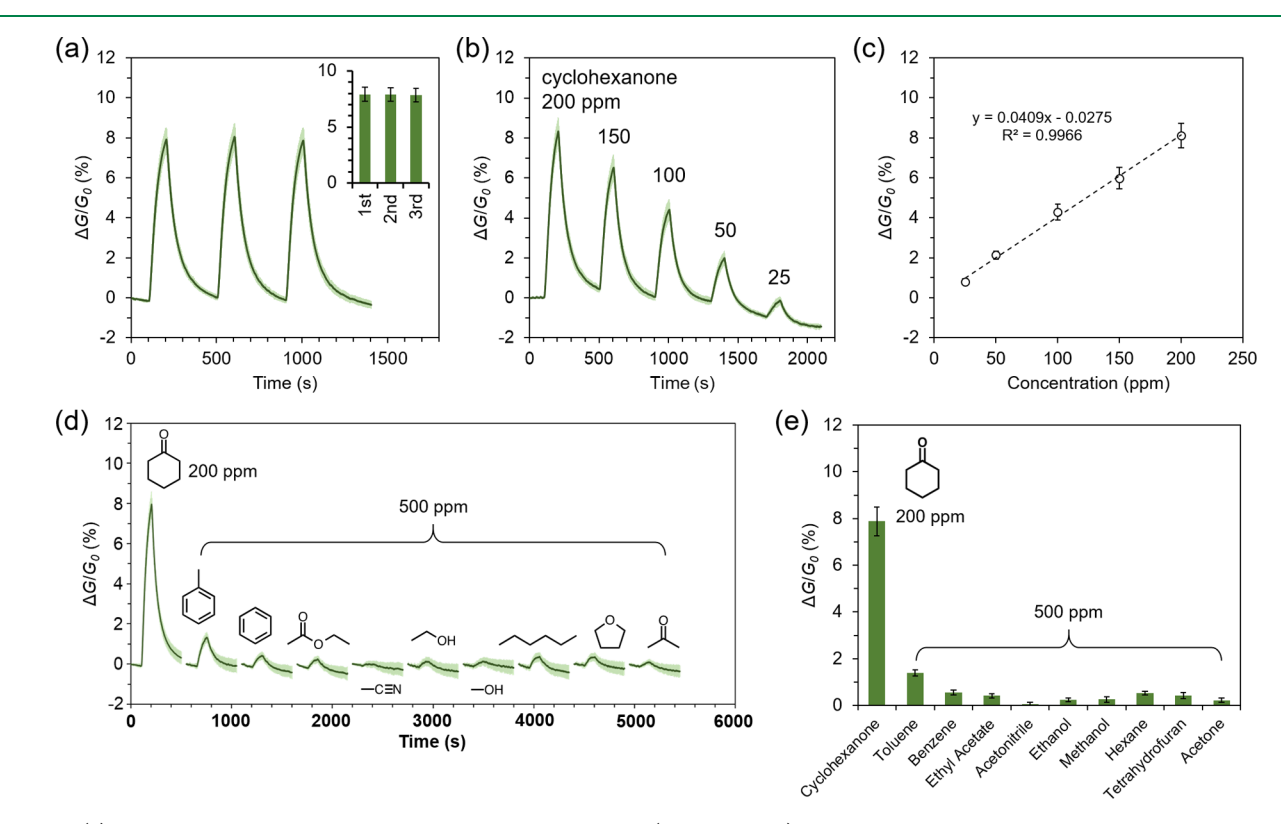


Figure 5. (a) Chemiresistive responses averaged over four devices of P(Q4VP-VBTU)-SWCNT in response to repeated 200 s exposure to 200 ppm cyclohexanone in N_2 . (b) Real-time average conductance traces and (c) average conductance responses of four P(Q4VP-VBTU)-SWCNT devices in response to 200 s exposure of varying concentrations of cyclohexanone in N_2 . (d) Real-time average conductance traces and (e) average conductance responses of four P(Q4VP-VBTU)-SWCNT devices in response to 200 s exposures of 200 ppm cyclohexanone and VOCs at a concentration of 500 ppm in N_2 .

P(Q4VP-VBTU)—SWCNT for cyclohexanone detection. Individual functionalization steps were confirmed by the attenuated total reflection-Fourier transform infrared (ATR-FTIR) spectroscopy (Figure 4a). After quaternization with bromoethane, P(Q4VP-VBAz)—SWCNT shows a shift of the pyridyl C=N stretching band to a higher frequency, from 1597 to 1640 cm⁻¹, and the characteristic azide band at around 2100 cm⁻¹ remains unchanged indicating orthogonal reactivity. The subsequent surface click reaction with TU was confirmed by the disappearance of the azide band, indicating the formation of P(Q4VP-VBTU)—SWCNT.²⁸

The two-step surface polymer-SWCNT functionalization was further investigated by XPS (Figure 4b-e). From the XPS survey scan of P(Q4VP-VBTU)-SWCNT, we observe characteristic peaks related to TU after the click addition including the N 1s, F 1s, and S 2p peaks, thereby supporting successful functionalization (Figure 4b). The separate functionalization steps were monitored by changes in the high-resolution N 1s spectrum. The N 1s spectrum of P(4VP-VBAz)-SWCNT displays a free pyridyl N peak at 398.9 eV (Figure 4c). Two distinctive peaks at 400.5 and 404.1 eV with a peak area ratio of 2:1 are attributed to the azide group.³ After the bromoethane treatment, the pyridyl N 1s peak shifts to the higher binding energy at 401.7 eV and the azide peaks are unchanged (Figure 4d). The quaternization yield is 95% based on the integrated areas of the N 1s peak at 398.9 eV for the residual pyridyl N and that at 401.7 eV for pyridinium N⁺ in P(Q4VP-VBAz)-SWCNT. Upon completion of the click reaction, two deconvoluted triazole N peaks at 400.5 and 402.6 eV are observed and the absence of the 404.1 eV peak corresponding to the azide group confirmed conversion to P(Q4VP-VBTU)-SWCNT (Figure 4e). In addition, a new N 1s peak centered at 399.7 eV corresponding to the thiourea N suggests that the TU has been added to the polymer-SWCNT composite.

A PET-APTES-BPTS substrate patterned with gold electrodes having an interelectrode spacing of 1 mm was functionalized by the sequential two-step surface treatment to immobilize P(Q4VP-VBTU)-SWCNT between the electrodes (Figure S3). We tested the resultant devices for their responses to 200 s exposures of 200 ppm cyclohexanone vapor diluted in dry N₂ (RH 0.1%), wherein the average baseline conductance (I_0) of four sensors is $0.9 \pm 0.6 \mu A$ (V = 3 V) at 22 °C. As shown in Figure 5a, the sensors exhibited an increase in conductance of 7.9 \pm 0.6% ($\Delta G/G_0$ (%) = $(I - I_0)/I_0 \times$ 100%) upon exposure to cyclohexanone. The conductance changes were investigated for cyclohexanone concentrations of 25–200 ppm in dry N_2 (Figure 5b,c). The experimental limit of detection was found to be 25 ppm with a linear response with respect to the concentration. The response ratio of the P(Q4VP-VBTU)-SWCNT sensor, dividing the change in conductance by the concentration in ppm $[(\Delta G/G_0)]$ (%))/ppm], shows an enhanced chemiresistive response of 0.041%/ppm compared to that of our previous sensors, 2.544 \times 10⁻⁵¹⁵ and 0.025%/ppm, ¹⁶ respectively, when tested under dry N2. Note that chemiresistive sensing cannot be performed solely with P(Q4VP-VBTU) as a result of the highly electrically resistive polymer. SWCNTs should be incorporated with P(Q4VP-VBTU) as an electrically conductive component to observe measurable chemiresistive sensing signals.

The conductance changes in the present study are in contrast to our previous thiourea-utilized sensors, wherein the decrease in conductance $(-\Delta G/G_0$ (%)) was observed in

response to cyclohexanone. ^{15,16} This feature suggests an enhanced hole density and/or mobility in the SWCNTs occurs with hydrogen bonding of the cyclohexanone to the TU. Such a change can infer a change in the collective dipole at the nanotube surface. ¹⁶ One feature that is different than previous sensors is that alkylated pyridiniums may play a role as well as the counterions.

The P(Q4VP-VBTU)–SWCNT sensors were also tested under dry (RH 5%) air as a carrier gas. Upon the exposure to air, the sensors exhibited a 1.6-fold increased baseline conductance ($I_0 = 1.5 \pm 0.8 \, \mu \text{A}$), which is mainly resulted from the adsorption of oxygen on the surface, which is known to inject hole carriers. When compared with the response in dry N₂, the sensors show slightly decreased conductance changes of 4.7 \pm 0.4% upon 200 s exposure to 200 ppm cyclohexanone (Figure S4), which is to be expected with an increased hole density in the SWCNT. Simply put there are more carriers, and the same amount of cyclohexanone will not be as effective at changing the population or mobility as is possible with less doping.

The effect on humidity was investigated using P(Q4VP-VBTU)-SWCNT sensors under humid (RH 55%) air as a carrier gas (Figure S4). In contrast to the dry conditions, the sensors exhibited a decrease in conductance $(-\Delta G/G_0$ (%)) upon exposure to cyclohexanone. This transition is likely related by the adsorption of water molecules on the SWCNT surface. In general, the adsorption of water results in a decrease in mobile hole concentration in CNTs as a result of electron donation (carrier compensation and pinning). Some of the water is likely in a hydrogen bonding complex with the TU, and cyclohexanone can in effect release the water to more preferably interact with the SWCNT. It should be noted that we lack enough information to be precisely sure about the mechanism of action, and the above discussion is a working hypothesis.

The selective cyclohexanone sensing of P(Q4VP-VBTU)-SWCNT sensors to the various VOCs is summarized in Figure 5d,e. Among the tested VOCs, the sensor exhibits high sensitivity and selectivity toward 200 ppm cyclohexanone over the other nine interfering analytes ($\Delta G/G_0 < 1.4\%$) even at higher concentrations of 500 ppm. This result confirms the utility of the strong hydrogen bonding in the TU-cyclohexanone complex. Although acetone has a carbonyl group that is capable of hydrogen-bonding interaction with thiourea NH protons, the sensor showed a higher binding affinity toward cyclohexanone. This feature reflects the reduced steric hindrance provided by the cyclic structure of cyclohexanone.

CONCLUSIONS

In summary, we developed a noncovalently functionalized SWCNT having thiourea (TU)-based selectors on a flexible PET substrate for selective detection of cyclohexanone. We first prepared a precursor wrapper polymer, that is, P(4VP-VBAz), composed of 4VP and azide groups. The wrapper polymer was utilized for the homogenous dispersion of SWCNTs to coat P(4VP-VBAz)—SWCNT on the PET film by spray-coating. Mechanically strong adhesion was achieved by the quaternization of 4VP groups with surface alkyl bromide groups on the treated PET substrates. Subsequently, the ketone-binding TU was added to the P(4VP-VBAz)—SWCNT by a "click" reaction to obtain the final P(Q4VP-VBTU)—SWCNT composite. P(Q4VP-VBTU)—SWCNT showed a substantial increase in conductance ($\Delta G/G_0$) of 7.9 \pm 0.6%

upon 200 s exposure to 200 ppm cyclohexanone vapor diluted in dry N_2 (RH 0.1%). The limit of detection was confirmed to be 25 ppm ($\Delta G/G_0=0.8\pm0.1\%$) with a response ratio ($\Delta G/G_0$ (%)/ppm) of 0.041%/ppm. The sensor exhibited stable cyclohexanone sensing property under dry air (RH 5%) with a slight decrease in response ($\Delta G/G_0=4.7\pm0.4\%$) toward 200 ppm cyclohexanone. Selective cyclohexanone sensing performance was achieved with minor responses ($\Delta G/G_0<1.4\%$ at 500 ppm) toward interfering VOCs. The surface functionalization technique of polymer–SWCNT composites on a flexible PET substrate provides a robust wearable gas-sensing platform that will find other applications.

ASSOCIATED CONTENT

Supporting Information

The Supporting Information is available free of charge at https://pubs.acs.org/doi/10.1021/acssensors.1c01076.

General materials; characterization; synthesis procedures; NMR spectra; and additional analysis data (PDF)

AUTHOR INFORMATION

Corresponding Authors

Timothy M. Swager — Institute for Soldier Nanotechnologies, Massachusetts Institute of Technology, Cambridge, Massachusetts 02139, United States; Department of Chemistry, Massachusetts Institute of Technology, Cambridge, Massachusetts 02139, United States; orcid.org/0000-0002-3577-0510; Email: tswager@mit.edu

Gary F. Walsh — Optical and Electromagnetic Materials Team, U.S. Army Combat Capabilities Development Command Soldier Center (DEVCOM SC), Natick, Massachusetts 01760, United States; Oorcid.org/0000-0003-2616-8939; Email: gary.f.walsh.civ@mail.mil

Authors

Bora Yoon — Optical and Electromagnetic Materials Team, U.S. Army Combat Capabilities Development Command Soldier Center (DEVCOM SC), Natick, Massachusetts 01760, United States; Institute for Soldier Nanotechnologies, Massachusetts Institute of Technology, Cambridge, Massachusetts 02139, United States; orcid.org/0000-0003-1338-7841

Seon-Jin Choi – Department of Chemistry, Massachusetts Institute of Technology, Cambridge, Massachusetts 02139, United States; Division of Materials of Science and Engineering, Hanyang University, Seoul 04763, Republic of Korea; ⊚ orcid.org/0000-0001-8567-0668

Complete contact information is available at: https://pubs.acs.org/10.1021/acssensors.1c01076

Author Contributions

[⊥]B.Y. and S.-J.C. contributed equally.

Note

The authors declare no competing financial interest.

■ ACKNOWLEDGMENTS

This work was sponsored by the Army Research Office through the Institute for Soldier Nanotechnologies and B.Y. was supported by an appointment to the Postgraduate Research Participation Program at the U.S. Army DEVCOM SC administered by the Oak Ridge Institute for Science and

Education through an interagency agreement between the U.S. Department of Energy and DEVCOM SC and the National Science Foundation DMR-1809740. This work was supported by the National Research Foundation of Korea (NRF) grant funded by the Korea government (MSIT) (no. 2020R1C1C1010336).

REFERENCES

- (1) United States Department of Homeland Security Explosives Detection Programs. https://www.dhs.gov/science-and-technology/explosives-division (accessed 11 May 2021).
- (2) United States Department of Homeland Security Secondary Screening Technology Development Program. https://www.dhs.gov/publication/secondary-screening-technology-development-program (accessed 11 May 2021).
- (3) Fainberg, A. Explosives Detection for Aviation Security. *Science* **1992**, 255, 1531–1537.
- (4) Senesac, L.; Thundat, T. G. Nanosensors for Trace Explosive Detection. *Mater. Today* **2008**, *11*, 28–36.
- (5) Lai, H.; Leung, A.; Magee, M.; Almirall, J. R. Identification of Volatile Chemical Signatures From Plastic Explosives by SPME-GC/MS and Detection by Ion Mobility Spectrometry. *Anal. Bioanal. Chem.* **2010**, *396*, 2997–3007.
- (6) Marder, D.; Tzanani, N.; Prihed, H.; Gura, S. Trace Detection of Explosives with a Unique Large Volume Injection Gas Chromatography-Mass Spectrometry (LVI-GC-MS) Method. *Anal. Methods* **2018**, *10*, 2712–2721.
- (7) To, K. C.; Ben-Jaber, S.; Parkin, I. P. Recent Developments in the Field of Explosive Trace Detection. *ACS Nano* **2020**, *14*, 10804–10833.
- (8) Germain, M. E.; Knapp, M. J. Optical Explosives Detection: From Color Changes to Fluorescence Turn-On. *Chem. Soc. Rev.* **2009**, 38, 2543–2555.
- (9) Kim, S.-J.; Choi, S.-J.; Jang, J.-S.; Cho, H.-J.; Kim, I.-D. Innovative Nanosensor for Disease Diagnosis. *Acc. Chem. Res.* **2017**, *50*, 1587–1596.
- (10) Cox, J. R.; Müller, P.; Swager, T. M. Interrupted Energy Transfer: Highly Selective Detection of Cyclic Ketones in the Vapor Phase. J. Am. Chem. Soc. 2011, 133, 12910–12913.
- (11) Askim, J. R.; Li, Z.; LaGasse, M. K.; Rankin, J. M.; Suslick, K. S. An Optoelectronic Nose for Identification of Explosives. *Chem. Sci.* **2016**, *7*, 199–206.
- (12) Liu, Y.-L.; Tseng, M.-C.; Chu, Y.-H. Sensing Ionic Liquids for Chemoselective Detection of Acyclic and Cyclic Ketone Gases. *Chem. Commun.* **2013**, *49*, 2560–2562.
- (13) Hu, Z.; Tan, K.; Lustig, W. P.; Wang, H.; Zhao, Y.; Zheng, C.; Banerjee, D.; Emge, T. J.; Chabal, Y. J.; Li, J. Effective Sensing of RDX via Instant and Selective Detection of Ketone Vapors. *Chem. Sci.* **2014**, *5*, 4873–4877.
- (14) Jaini, A. K. A.; Hughes, L. B.; Kitimet, M. M.; Ulep, K. J.; Leopold, M. C.; Parish, C. A. Halogen Bonding Interactions for Aromatic and Nonaromatic Explosive Detection. *ACS Sens.* **2019**, *4*, 389–397
- (15) Schnorr, J. M.; van der Zwaag, D.; Walish, J. J.; Weizmann, Y.; Swager, T. M. Sensory Arrays of Covalently Functionalized Single-Walled Carbon Nanotubes for Explosive Detection. *Adv. Funct. Mater.* **2013**, 23, 5285–5291.
- (16) Frazier, K. M.; Swager, T. M. Robust Cyclohexanone Selective Chemiresistors Based on Single-Walled Carbon Nanotubes. *Anal. Chem.* **2013**, *85*, 7154–7158.
- (17) Cho, S. H.; Suh, J. M.; Eom, T. H.; Kim, T.; Jang, H. W. Colorimetric Sensors for Toxic and Hazardous Gas Detection: A Review. *Electron. Mater. Lett.* **2021**, *17*, 1–17.
- (18) Schroeder, V.; Savagatrup, S.; He, M.; Lin, S.; Swager, T. M. Carbon Nanotube Chemical Sensors. *Chem. Rev.* **2019**, *119*, 599–663.
- (19) Kauffman, D. R.; Star, A. Carbon Nanotube Gas and Vapor Sensors. *Angew. Chem., Int. Ed.* **2008**, *47*, 6550–6570.

- (20) Hwang, S. I.; Franconi, N. G.; Rothfuss, M. A.; Bocan, K. N.; Bian, L.; White, D. L.; Burkert, S. C.; Euler, R. W.; Sopher, B. J.; Vinay, M. L.; Sejdic, E.; Star, A. Tetrahydrocannabinol Detection Using Semiconductor-Enriched Single-Walled Carbon Nanotube Chemiresistors. ACS Sens. 2019, 4, 2084—2093.
- (21) Choi, S.-J.; Choi, H.-J.; Koo, W.-T.; Huh, D.; Lee, H.; Kim, I.-D. Metal-Organic Framework-Templated PdO-Co₃O₄ Nanocubes Functionalized by SWCNTs: Improved NO₂ Reaction Kinetics on Flexible Heating Film. ACS Appl. Mater. Interfaces **2017**, *9*, 40593–40603.
- (22) Bezdek, M. J.; Luo, S.-X. L.; Ku, K. H.; Swager, T. M. A Chemiresistive Methane Sensor. *Proc. Natl. Acad. Sci. U.S.A.* **2021**, 118, No. e2022515118.
- (23) Hwang, S. I.; Chen, H.-Y.; Fenk, C.; Rothfuss, M. A.; Bocan, K. N.; Franconi, N. G.; Morgan, G. J.; White, D. L.; Burkert, S. C.; Ellis, J. E.; Vinay, M. L.; Rometo, D. A.; Finegold, D. N.; Sejdic, E.; Cho, S. K.; Star, A. Breath Acetone Sensing Based on Single-Walled Carbon Nanotube-Titanium Dioxide Hybrids Enabled by a Custom-Built Dehumidifier. ACS Sens. 2021, 6, 871–880.
- (24) Saem, S.; Fong, D.; Adronov, A.; Moran-Mirabal, J. Stretchable and Resilient Conductive Films on Polydimethylsiloxane from Reactive Polymer-Single-Walled Carbon Nanotube Complexes for Wearable Electronics. ACS Appl. Nano Mater. 2019, 2, 4968–4973.
- (25) Yoon, B.; Liu, S. F.; Swager, T. M. Surface-Anchored Poly(4-vinylpyridine)-Single-Walled Carbon Nanotube Metal Composites for Gas Detection. *Chem. Mater.* **2016**, *28*, 5916–5924.
- (26) Zhu, R.; Desroches, M.; Yoon, B.; Swager, T. M. Wireless Oxygen Sensors Enabled by Fe(II)-Polymer Wrapped Carbon Nanotubes. ACS Sens. 2017, 2, 1044–1050.
- (27) Soylemez, S.; Yoon, B.; Toppare, L.; Swager, T. M. Quaternized Polymer-Single-Walled Carbon Nanotube Scaffolds for a Chemiresistive Glucose Sensor. ACS Sens. 2017, 2, 1123–1127.
- (28) Yoon, B.; Choi, S.-J.; Swager, T. M.; Walsh, G. F. Switchable Single-Walled Carbon Nanotube-Polymer Composites for CO₂ Sensing. ACS Appl. Mater. Interfaces 2018, 10, 33373–33379.
- (29) Choi, S.-J.; Yoon, B.; Lin, S.; Swager, T. M. Functional Single-Walled Carbon Nanotubes for Anion Sensing. *ACS Appl. Mater. Interfaces* **2020**, *12*, 28375–28382.
- (30) Choi, S. J.; Yoon, B.; Ray, J. D.; Netchaev, A.; Moores, L. C.; Swager, T. M. Chemiresistors for the Real-Time Wireless Detection of Anions. *Adv. Funct. Mater.* **2020**, *30*, 1907087.
- (31) Fadeev, A. Y.; McCarthy, T. J. Surface Modification of Poly(ethylene terephthalate) to Prepare Surfaces with Silica-Like Reactivity. *Langmuir* **1998**, *14*, 5586–5593.
- (32) Castillo, G. A.; Wilson, L.; Efimenko, K.; Dickey, M. D.; Gorman, C. B.; Genzer, J. Amidation of Polyesters Is Slow in Nonaqueous Solvents: Efficient Amidation of Poly(ethylene terephthalate) with 3-Aminopropyltriethoxysilane in Water for Generating Multifunctional Surfaces. ACS Appl. Mater. Interfaces 2016, 8, 35641–35649.
- (33) Bùi, L. N.; Thompson, M.; Mckeown, N. B.; Romaschin, A. D.; Kalman, P. G. Surface Modification of the Biomedical Polymer Poly(Ethylene-Terephthalate). *Analyst* **1993**, *118*, 463–474.
- (34) Özçam, A. E.; Roskov, K. E.; Spontak, R. J.; Genzer, J. Generation of Functional PET Microfibers through Surface-Initiated Polymerization. *J. Mater. Chem.* **2012**, 22, 5855–5864.
- (35) Gouget-Laemmel, A. C.; Yang, J.; Lodhi, M. A.; Siriwardena, A.; Aureau, D.; Boukherroub, R.; Chazalviel, J.-N.; Ozanam, F.; Szunerits, S. Functionalization of Azide-Terminated Silicon Surfaces with Glycans using Click Chemistry: XPS and FTIR Study. *J. Phys. Chem. C* 2013, 117, 368–375.
- (36) Qiu, J.; Zhou, X.; Mo, Q.; Liu, F.; Jiang, L. Electrostatic Assembled of Keggin-Type Polyoxometalates onto Poly(4-vinyl-pyridine)-Grafted Poly(vinylidene Fluoride) Membranes. *RSC Adv.* **2014**, *4*, 48931–48937.
- (37) Collins, P. G.; Bradley, K.; Ishigami, M.; Zettl, A. Extreme Oxygen Sensitivity of Electronic Properties of Carbon Nanotubes. *Science* **2000**, 287, 1801–1804.

- (38) Bradley, K.; Jhi, S.-H.; Collins, P. G.; Hone, J.; Cohen, M. L.; Louie, S. G.; Zettl, A. Is the Intrinsic Thermoelectric Power of Carbon Nanotubes Positive? *Phys. Rev. Lett.* **2000**, *85*, 4361–4364.
- (39) Na, P. S.; Kim, H.; So, H.-M.; Kong, K.-J.; Chang, H.; Ryu, B. H.; Choi, Y.; Lee, J.-O.; Kim, B.-K.; Kim, J.-J.; Kim, J. Investigation of the Humidity Effect on the Electrical Properties of Single-Walled Carbon Nanotube Transistors. *Appl. Phys. Lett.* **2005**, *87*, 093101.
- (40) Zahab, A.; Spina, L.; Poncharal, P.; Marlière, C. Water-Vapor Effect on the Electrical Conductivity of a Single-Walled Carbon Nanotube Mat. *Phys. Rev. B: Condens. Matter Mater. Phys.* **2000**, *62*, 10000–10003.
- (41) Watts, P. C. P.; Mureau, N.; Tang, Z.; Miyajima, Y.; Carey, J. D.; Silva, S. R. P. The Importance of Oxygen-Containing Defects on Carbon Nanotubes for the Detection of Polar and Non-Polar Vapours through Hydrogen Bond Formation. *Nanotechnology* **2007**, *18*, 175701.
- (42) Kim, W.; Javey, A.; Vermesh, O.; Wang, Q.; Li, Y.; Dai, H. Hysteresis Caused by Water Molecules in Carbon Nanotube Field-Effect Transistors. *Nano Lett.* **2003**, *3*, 193–198.